Arab J Sci Eng (2016) 41:3995–4005
DOI 10.1007/s13369-016-2064-z

RESEARCH ARTICLE - CIVIL ENGINEERING

Characteristics of Cyclic Shear Behavior of Sandy Soils: A Laboratory Study

A. Krim[1,2] · A. Arab[2] · R. Bouferra[3] · M. Sadek[4] · I. Shahrour[4]

Received: 28 November 2014 / Accepted: 11 February 2016 / Published online: 4 March 2016

Abstract This paper presents a laboratory study of the influence of relative density on the liquefaction potential of a sandy soil using the triaxial apparatus. The study is based on undrained triaxial tests performed on samples at an initial relative density RD = 15, 50 and 65 % under a confining pressure of 100 kPa using a dry deposition method. Samples were subjected to quasi-static undrained cyclic tests. The paper is composed of three parts. In the first part the used materials and their characteristics are presented. The second part is devoted to the experimental procedures and the device used. The third part investigates the influence of relative density on the liquefaction potential of the three sands (Hostun Rf, Chlef and Rass). This study also explores the influence of particle size on the liquefaction potential. The test results indicate that consistent results were obtained and show clearly that increasing the relative density leads to an important improvement in the liquefaction resistance of sand. This effect is very pronounced when the initial relative density increases from 50 to 65 %.

Keywords Undrained behavior · Cyclic loading · Confining pressure · Sand density · Liquefaction resistance · Static loading

✉ A. Arab
ah_arab@yahoo.fr

1 Ibn Khaldoun University, 14000 Tiaret, Algeria

2 Laboratory of Materials Sciences and Environment, Hassiba Ben Bouali University, 2000 Chlef, Algeria

3 Faculty of Science and Technology, Marrakech, Morocco

4 Laboratory of Civil Engineering and geo-Environment (LGCgE), USTLille1, Lille, France

List of symbols

ρ_s	Specific density of the solid grains
D_{10}	Effective grain diameter
D_{50}	Mean grain size of sand
D	Initial diameter of sample
C_u	Coefficient of uniformity ($C_u = D_{60}/D_{10}$)
CSR	Cyclic stress ratio (CSR $= q_m/2 \cdot p_c'$)
e_{max}	Maximum void ratio
e_{min}	Minimum void ratio
H	Initial height of sample
N_c	Number of cycles
RD	Relative density
p_c'	Initial effective confining pressure
q	Deviator stress
P'	Effective mean pressure
q_m	Cyclic loading amplitude
Δu	Excess pore pressure
ε_a	Axial strain
UTH	Undrained test of Hostun sand
UTR	Undrained test of Rass sand
UTC	Undrained test of Chlef sand

1 Introduction

The liquefaction resistance of a specific sandy site subjected to a high risk of liquefaction can be improved if action is taken to change one or more of the influencing parameters. Currently, most methods used for the stabilization sites do affect the relative density and drainage conditions of the soil. Recently, new methods of stabilizing liquefiable sites were considered. These methods intended to improve the liquefaction resistance by inclusion of geotextile webs and by increasing the permeability of the soil. The relative density

affects very significantly the potential of soil liquefaction (Mohamad and Dobry [1]; Konrad [2]; Hyodo et al. [3]). Figure 1 shows the results obtained by Tatsuoka et al. [4] on Toyoura sand. It was found that the liquefaction resistance increases linearly with the relative density until a value of relative density of RD = 70 % is reached. After this value, we note a significant increase in liquefaction resistance with the increase in the relative density.

Finn et al. [5] investigated the influence of loading path on the liquefaction resistance of sands. They found that this resistance increases when the soil sample is subjected to a small cyclic loading followed by drainage.

Belkhatir et al. [6] studied the influence of relative density on the liquefaction resistance of Chlef sand-silt mixtures, by performing a series of undrained cyclic triaxial tests on sand-silt mixtures mixed with a fines content of 5 % for two relative densities of: RD = 12 and 60 %. They found that the increase in the relative density leads to an increase in the liquefaction resistance of Chlef sand-silt mixture. Another undrained cyclic tests were performed by Belkhatir et al. [7] on Chlef sand with different fines ranging from 0 to 40 % for a relative density of RD = 50 %. They found that liquefaction resistance of the sand-silt mixture decreases with increase in the fines content, consequently to an increase in the risk of liquefaction.

Polito and Martin [8] have conducted a series of triaxial tests on sand samples (Monterrey and Yatesville sands) mixed with 0–100 % of non-plastic fines. They noticed a linear tendency between the increase in relative density and the increase in liquefaction resistance for samples with fines content until a limiting value of fines content is reached. However, the liquefaction resistance above a certain limiting value is also controlled by the relative density of the sample. This limiting value of fines content tends to fall between 35 and 55 %.

In this paper, we present a laboratory study on the influence of relative density on the liquefaction resistance of selected sandy soils. These tests provide a good knowledge on the influence of relative density on the cyclic behavior of sands. The paper is composed of three parts: In the first part, the used materials are presented. The second part is devoted to the experimental procedures and the device used for the cyclic tests. The last part provides an analysis of the experimental test results and discusses the influence of relative density on the cyclic behavior of sands.

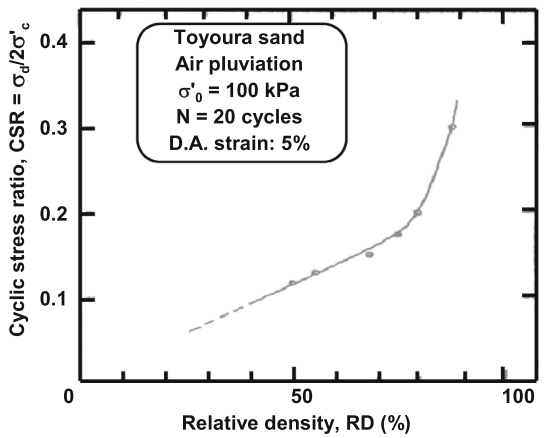

Fig. 1 Effect of density on the liquefaction resistance of Toyoura sand (Tatsuoka et al. [4])

2 Laboratory Testing

2.1 Materials Tested

Three materials were used in this study namely: Rass sand, Chlef sand (Algeria), and the Hostun Rf sand (France). Figure 2 shows the scanning electron microscope (SEM) view of tested sands. Chlef sand, as the name suggests, comes from the Oued Chlef which crosses the city of Chlef. The Rass sand comes from the Oued Rass (confluence of Oued Chlef and Oued Rass). The Hostun Rf sand comes from SIKA plants located near Hostun (Drôme, France). It arose from a thick series of Eocene sand layers that fill karst pockets on the western side of Vercors at Hostun (Drôme, France). Chlef sand

Fig. 2 Scanning electron microscope (SEM) view of tested sands: Showing particle's size and shape. **a** Chlef (Belkhatir et al. [6]), **b** Rass (Krim et al. [12]), **c** Hostun Rf (Benahmed et al. [13])

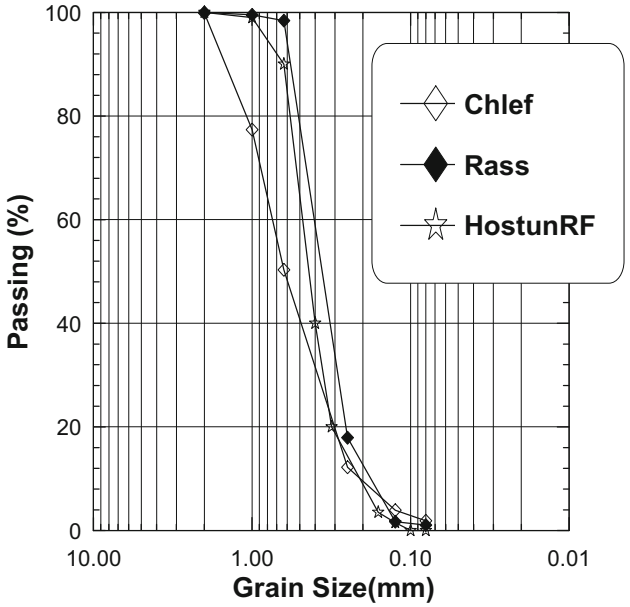

Fig. 3 Grain size distribution curves of tested sands (Chlef, Rass and Hostun Rf)

is a medium sand with rounded grains (alluvial sand) and a medium diameter of: $D_{50} = 0.61$ mm (Della and Arab [9]; Belkhatir et al. [10]). Rass sand is also a rounded sand (alluvial sand) with a medium diameter of $D_{50} = 0.39$ mm (Arab [11]; Krim et al. [12]). Hostun Rf sand is considered a reference material in many laboratories in France (Benahmed et al. [13]). Numerous tests were carried out on this sand (Colliat [14]; Fargeix [15]; Flavigny et al. [16]; Biarez and Ziani [17]; Lancelot et al. [18]; Doanh et al. [19]; Al Mahmoud [20]; Hoque and Tatsuoka [21]). This is a medium sand with angular grains and a medium diameter of $D_{50} = 0.471$ mm. Figure 3 shows the grain size distribution curves of the tested materials. The principal properties and the chemical analysis of these sands are summarized in a Tables 1 and 2.

Table 1 Principal properties of tested sands (Chlef, Rass and Hostun Rf)

Properties	Sand		
	Chlef	Rass	Hostun Rf
ρ_s (g/cm^3)	2.68	2.664	2.654
e_{max}	0.854	0.770	0.983
e_{min}	0.535	0.490	0.622
$C_u = (D_{60}/D_{10})$	3.38	2.42	2.27
D_{10} (mm)	0.225	0.227	0.19
D_{50} (mm)	0.61	0.39	0.471
Particle shape	Rounded	Rounded	Angular
Color	Gray white	Clear brown	Gray white to pinkish beige
Fabric	River sand	River sand	Artificial sand

Table 2 Chemical analysis of tested sands (Chlef, Rass and Hostun Rf) (Arab et al. [11])

Composition (%)	Sand		
	Chlef	Rass	Hostun Rf
Fire loss	14.34	6.23	0.55
Total silica (SiO_2)	55.89	78.20	99.17
Alumina (Al_2O_3)	5.58	2.03	0.25
Oxide of iron (Fe_2O_3)	7.58	5.58	0.17
Oxide of titane (TiO_2)	0.00	0.00	0.01
Lime (CaO)	15.42	8.13	0.14
Magnesia (MgO)	0.00	0.00	0.14
Potash (K_2O)	Traces	Traces	0.02
Oxide of sodium (Na_2O)	Traces	Traces	0.05
Sulfates SO_4	0.28	0.24	0.00
Chlorides CL-Solubles in water	0.14	0.14	0.00
Carbonates $CaCO_3$	24.60	13.94	0.00
Insolubles	0.53	0.93	0.00
Organic materials	0.00	0.00	0.00

2.2 Experimental Device Used

The experimental device used is shown schematically in Fig. 4. It contains:

(a) A triaxial cell of Wesley Bishop type (Bishop and Wesley [22]),
(b) Three controllers of the pressure/volume type GDS (200cc),
(c) A void pump connected to a reservoir in order to de-air the demineralized water,
(d) And, all the measurements are recorded using a data acquisition system under computer control.

The triaxial cell consists of two tubes. The upper one contains the sample and the two bases for applying the axial load on the sample. The maximum capacity of this press is 2 MPa. The lower part consists of a hydraulic press. The hydraulic press consists of a steel tube in which a piston can slide. The end of the piston is connected to the lower base applying the axial load to the sample. The controllers regulate, accurately, pressure and volume change of deaerated water supplied to the cell to control: axial load or axial deformation, cell pressure, and back pressure. A controller (GDS n1) of the pressure is connected to the cell for applying a confining pressure; another GDS n2 is connected to the drained circuit, and this controller is a hydraulic pump controlled

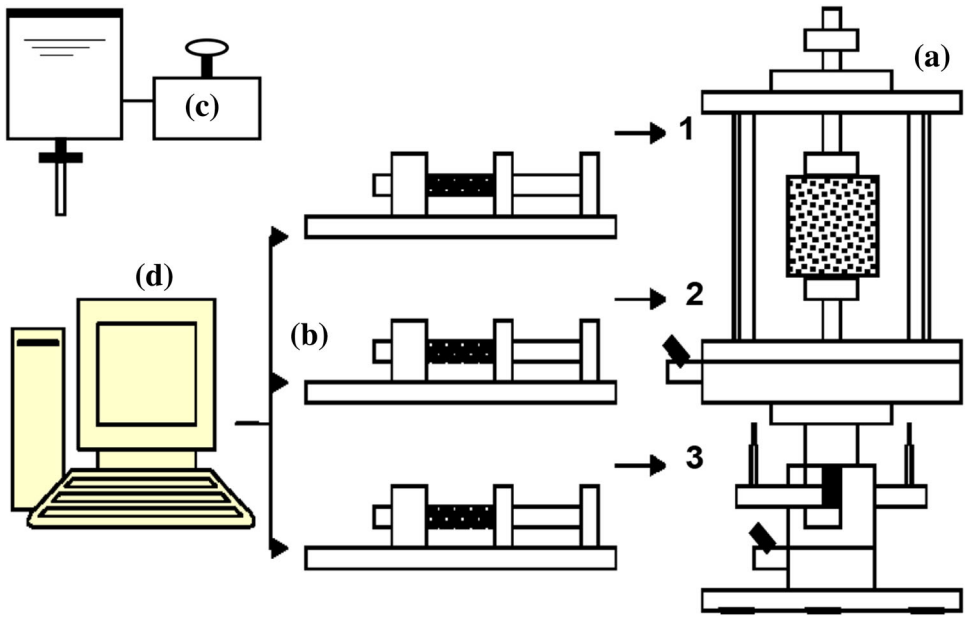

Fig. 4 Experimental devise for the cyclic tests. *1*) Application of pressure in the cell; *2*) Control of interstitial pressure and variation of sample's volume; *3*) Deviator control, *a*) A triaxial cell, *b*) Three controllers of the pressure/volume, *c*) Void pump, *d*) Computer

by a computer, which is used to adjust and to measure the pressure and volume change of the fluid. The filling of the cell and the saturation of the sample were carried out using a perspex reservoir containing a demineralized, and deaeration of water was performed with a vacuum pump. Pore pressure was measured by the back-pressure controller. The digital controllers, pore pressure indicator, axial deformation, axial loading indicator, and printer are connected to the computer to insure proper data acquisition of tests.

2.3 Specimen Preparation and Depositional Technique

Dry funnel pluviation was used to reconstitute the samples. The samples were prepared using a mold consisting of two semicylinders, which are assembled and tightened by a collar. The two semicylinders are used to set up the latex membrane in the mold. In order to simulate a relatively homogeneous soil condition, under-compaction method of sample preparation was used. The sample was prepared in seven layers of increasing relative density from the bottom to the top. The method recommended by Ladd [23] was modified by Chan [24], who recommends a difference of relative density of one percent between two successive layers. The dry soil is compacted in seven layers. As each layer is placed inside the mold, some of the compaction energy will be transmitted to the lower layers. Therefore, not only the layer being placed would be affected, but also the layers below it are likely to be densified. To compensate for this, the layers were compacted at an increasing relative density from the bottom to the top. For example, if an overall relative density of 50 % is desired, then seven layers would be placed from the bottom to the top at relative densities of: 47, 48, 49, 50, 51, 52, and 53 % respectively. After the sample cap has been formed, the sample is placed and sealed with two O-rings, and a partial vacuum of 15–25 kPa is applied to the sample to reduce the disturbance of the sample. The two semicylinders can be easily assembled or separated using a tightening collar. In order to maintain the latex membrane along the face of the mold, four ducts of aspiration were perforated in the semicylinders. These ducts communicate with the inside of the mold by rows of small holes (1 mm of diameter). These rows are connected to flexible pipes and assembled in a single tube. This tube was connected to a vacuum pomp. Cylindrical soil samples had a diameter (D) of 70 mm and a height (H) of 140 mm. Consequently, test samples had an $(H/D)=2$, and, in general, were with smooth lubricated end-plates. The mass of sand to be placed in the mold depends on the required density where the initial volume of the sample is known, and the density state of the sample was defined by the relative density (RD):

$$\mathrm{RD} = (e_{\max} - \mathrm{e})/(e_{\max} - e_{\min}) \quad (1)$$

where $e_{\min}$ and $e_{\max}$ are the minimum and the maximum void ratios, respectively; e is the intended void ratio, and RD is relative density.

2.4 Saturation and Consolidation of the Sample

Saturation is an important stage in the experimental procedure because the response of the sample under undrained loading depends on the degree of saturation. In order to ensure a good saturation, the samples were saturated by injecting CO_2 gas during a 20-min period under a low pressure of 15 kPa (Lade and Duncan [25]), followed by injection of deaerated water after which deaerated and demineralized water are injected. The application of a back pressure of 500 kPa, using the GDS n2, improves the quality of satura-

tion, by compressing the microbubbles of the interstitial gas that can still be present after the saturation phase. These two pressures (in the cell and inside the sample) were maintained during a whole night prior to testing, until the volume is stable, to ensure good consolidation. Samples were isotropically consolidated with an initial effective confining pressure of 100 kPa, which is equivalent to the in situ effective stress where the soil sample was collected from.

The quality of saturation is evaluated with a measure of the Skempton's coefficient (B), according to a classic process: An increment $\Delta\sigma$ of the confining pressure of 100 kPa in an undrained condition is applied, and the response of the interstitial pressure Δu is measured and the degree of saturation of tested samples are evaluated by measuring Skempton's coefficient after consolidation by the formula: $B = \Delta u/\Delta\sigma$, where B value of at least 0.99 is either used or measured to indicate full saturation. It is noted that saturation affects significantly the shear strength of soils and the liquefaction resistance of sands increases when the degree of saturation decreases (Arab et al. [26]).

2.5 Shear Loading

All undrained triaxial tests for this study were carried out at a constant strain rate of 0.167 % per minute, which was slow enough to allow pore pressure change to equalize throughout the sample, with the pore pressure measured at the base of the sample.

3 Results and Discussions

We present below the results of undrained cyclic triaxial tests designed to study the effect of the initial relative density and cyclic loading levels on the liquefaction potential of three sands (Hostun Rf, Rass sand, and Chlef sand). A frequency of 0.5 Hz was used through out the testing program. The experimental program has selected three initial relative densities. The selected relative densities were: 15, 50, and 65 % respectively, with the same confining pressure of 100 kPa. For each relative density, tests were conducted at different loading amplitudes or loading levels (CSR) in order to draw the liquefaction potential curves. Table 3 summarizes the results of the undrained cyclic compression triaxial tests. The cyclic loading level or cyclic stress ratio (CSR) was defined as:

$$\mathrm{CSR} = q_\mathrm{m}/2 \cdot p'_\mathrm{c} \tag{2}$$

where q_m and p'_c are the cyclic loading amplitude and the initial effective confining pressure, respectively.

For a loose sand of RD = 15 %, tests were conducted for three amplitudes of 60, 40, and 30 kPa for Hostun Rf sand and 70, 50, and 30 kPa for Rass and Chlef sand. It was noted that the liquefaction was reached quickly for the high loading amplitude, whereas the liquefaction under at low loading amplitude took a relatively higher number of cycles. As shown in Table 3.

Table 3 Summary of undrained cyclic triaxial tests

Sand	Test No	RD (%)	p'_c (kPa)	q_m (kPa)	CSR = $q_\mathrm{m}/2.p'_\mathrm{c}$	Number of cycles
Hostun Rf	UTH1	15	100	60	0.30	2
	UTH2	15	100	40	0.20	3
	UTH3	15	100	30	0.15	18
	UTH4	50	100	70	0.35	7
	UTH5	50	100	60	0.30	9
	UTH6	50	100	50	0.25	8
	UTH7	50	100	40	0.20	20
	UTH8	50	100	30	0.15	87
	UTH9	65	100	70	0.35	10
	UTH10	65	100	50	0.25	12
	UTH11	65	100	40	0.20	60
	UTH12	65	100	30	0.15	92
Rass	UTR13	15	100	70	0.35	1
	UTR14	15	100	50	0.25	2
	UTR15	15	100	30	0.15	15
	UTR16	50	100	70	0.35	2
	UTR17	50	100	50	0.25	4
	UTR18	50	100	30	0.15	51
	UTR19	65	100	70	0.35	9
	UTR20	65	100	50	0.25	12
	UTR21	65	100	30	0.15	176
Chlef	UTC22	15	100	70	0.35	2
	UTC 23	15	100	50	0.25	2
	UTC24	15	100	30	0.15	22
	UTC25	50	100	70	0.35	4
	UTC26	50	100	50	0.25	5
	UTC27	50	100	30	0.15	80
	UTC28	65	100	70	0.35	8
	UTC29	65	100	50	0.25	12
	UTC30	65	100	30	0.15	140

For a medium sand of RD = 50 %, tests were also carried out for five loading amplitudes of 70, 60, 50, 40, and 30 kPa for Hostun Rf sand and 70, 50, and 30 kPa for Rass and Chlef sand. As noted in these test results, this density requires a higher number of cycles for the arrival to total liquefaction as compared with the tests of loose sand. As shown in Table 3. Typical test results of Hostun Rf sand are presented in Fig. 5 for a relative density of 50 % with a loading amplitude of 40 kPa, liquefaction occurred after 20 cycles.

For a higher relative density of RD = 65 %, tests were also performed for loading amplitudes of 70, 50, 40, and 30 kPa for Hostun Rf sand and 70, 50, and 30 kPa for Rass and Chlef

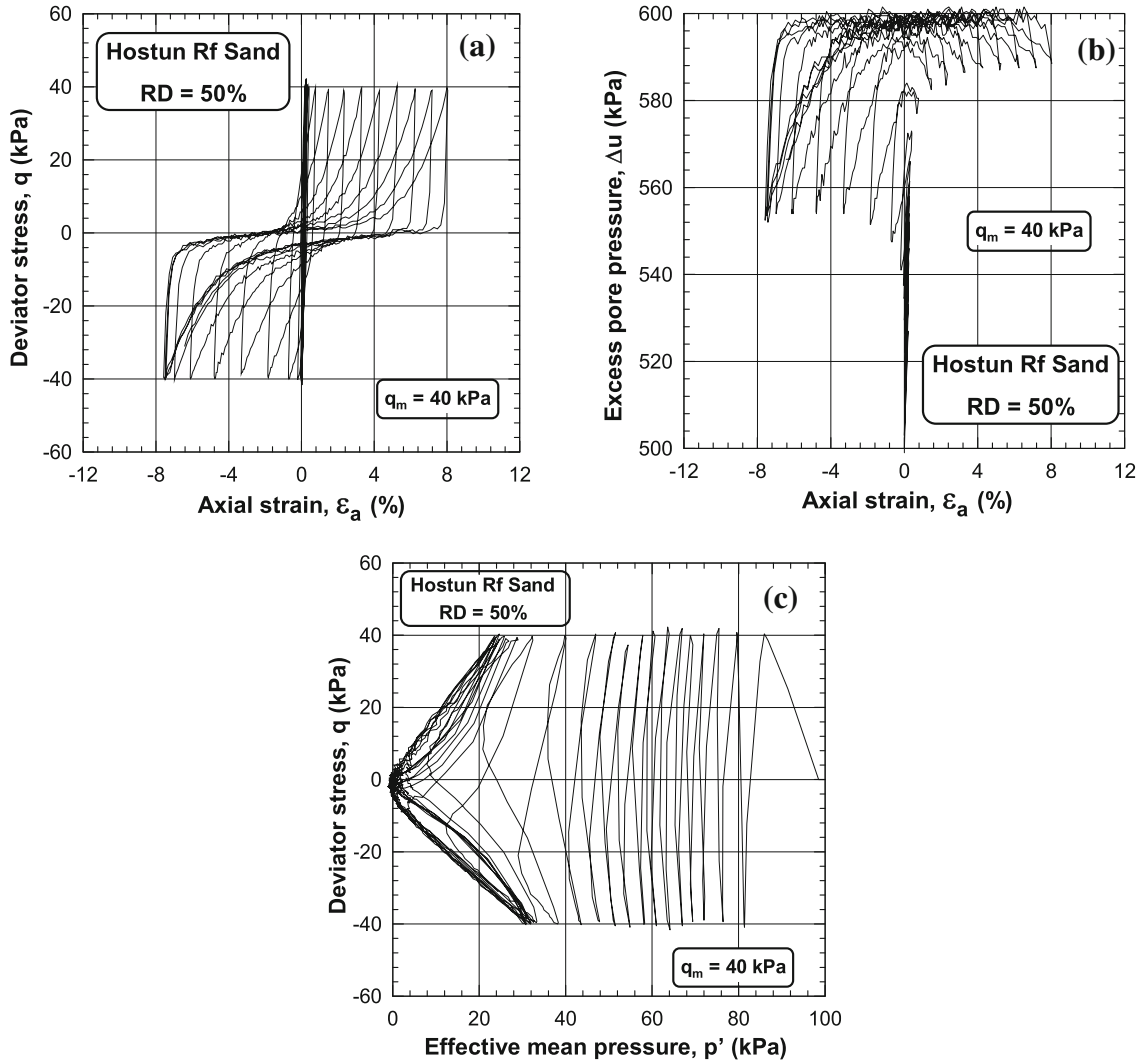

Fig. 5 Undrained cyclic tests on Hostun Rf sand (RD = 50 %, $p'_c = 100$ kPa, $q_m = 40$ kPa). **a** Deviator stress (q) versus axial strain (ε_a), **b** excess pore pressure (Δu) versus axial strain (ε_a), **c** deviator stress (q) versus effective mean pressure (p')

sand. As also noted in these test results, this higher density requires an even higher number of cycles for a complete liquefaction in comparison with tests carried out at the densities of RD = 15 and 50 %. Similar results were obtained for the other loading amplitudes. As shown in Table 3.

Figure 6 shows the variation of the excess pore pressure and the axial strain versus the number of cycles for the three relative densities of RD = 15, 50 and 65 % for the Hostun Rf sand. For the three relative densities of RD = 15, 50, and 65 %, Fig. 6a shows clearly the increase in the rate of the pore pressure with the increase in the number of cycles, and this increase is very significant for low loading amplitudes q_m. However, we note an important development of the excess pore pressure when q_m increases from 30 to 70 kPa. Also, as noted in Fig. 6b, axial strains for the loose and medium dense sand (RD = 15 and 50 %) increase rapidly at low number of cycles. Additionally, and as noted in Fig. 6b, resulting axial strains at RD = 65 %, are considerably less than those of lower RD's, namely: RD = 15 and 50 %.

Figures 7, 8, and 9 illustrate also the variation of excess pore pressure and the axial strain versus time for the three relative densities of RD = 15, 50 and 65 % for the Rass sand. These figures show an increase in the excess pore pressure with the increase of cyclic loading amplitude (q_m). This increase is more pronounced when q_m increases from 30 to 70 kPa. Also, axial strain increases with the increase of q_m.

We note that the test with CSR = 0.35 generates the excess pore pressure rather rapidly reaching a value of 588 kPa after one cycle for RD = 15 % (Fig. 7a); for RD = 50 %, the test took a longer time than the first (RD = 15 %) to generate the excess pore pressure after two cycles (Fig. 8a), for RD = 65 %, the test generated the excess pore pressure after nine cycles (Fig. 9a). The axial strain reached was 1.2 % in compression and 17 % in extension for RD = 15 % (Fig. 7b), 2.2 % in

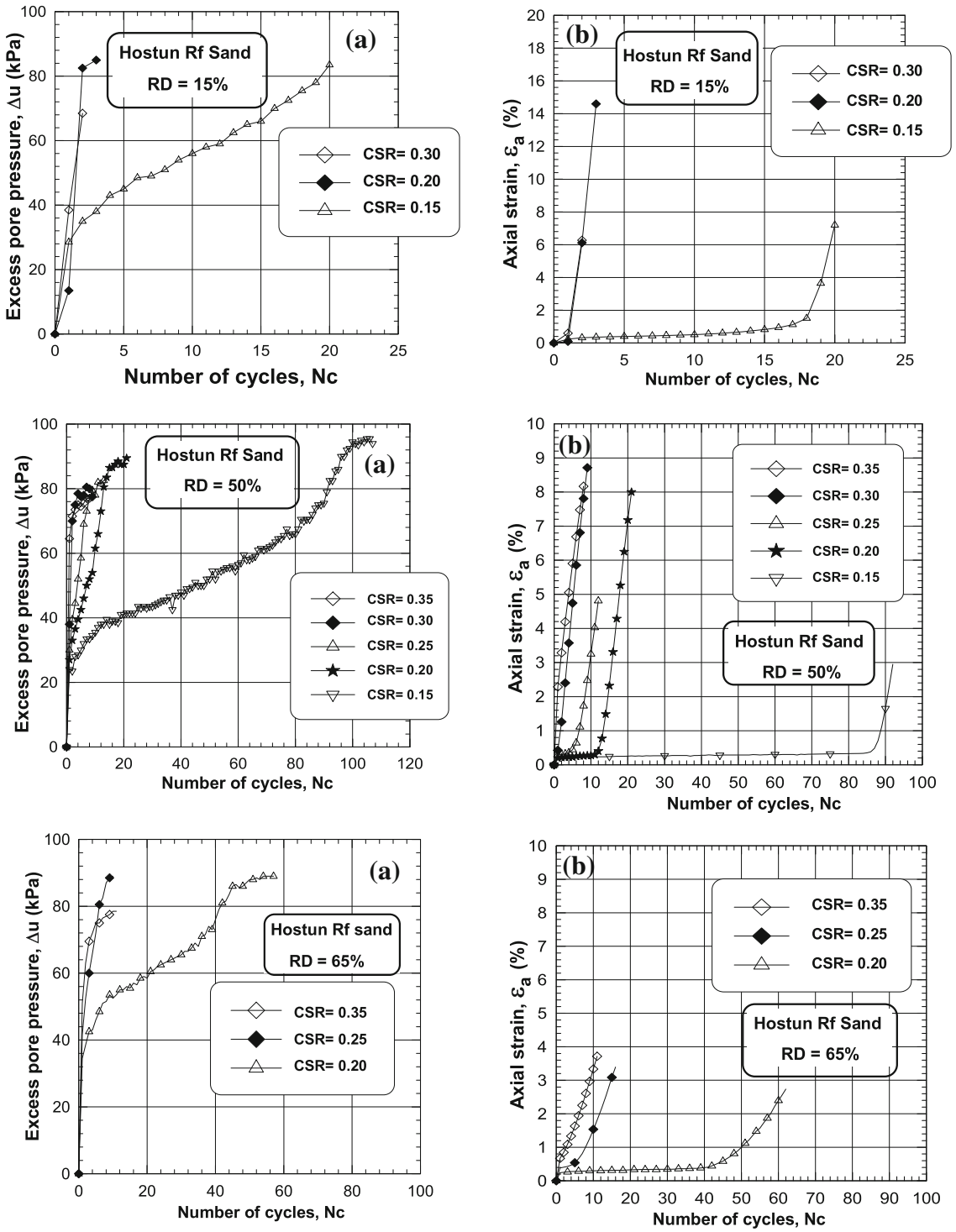

Fig. 6 Influence of loading amplitude on undrained behavior of Hostun Rf sand (RD = 15, 50 and 65 %, $p'_c = 100$ kPa). **a** Excess pore pressure (Δu) versus number of cycles (N_c), **b** axial strain (ε_a) versus number of cycles (N_c)

compression and 6 % in extension for RD = 50 % (Fig. 8b) and 2.5 % in compression and 3.5 % in extension for RD = 65 % (Fig. 9b).

The test with CSR = 0.25 also took a longer time to generate the excess pore pressure reaching the value of the cell pressure (600 kPa) after two cycles for RD = 15 % (Fig. 7a). For RD = 50 %, the test generates the excess pore pressure quickly reaching the cell pressure (600 kPa) after four cycles resulting in zero effective stress (Fig. 8a). For RD = 65 %, the test took also more time to generate the excess pore pressure

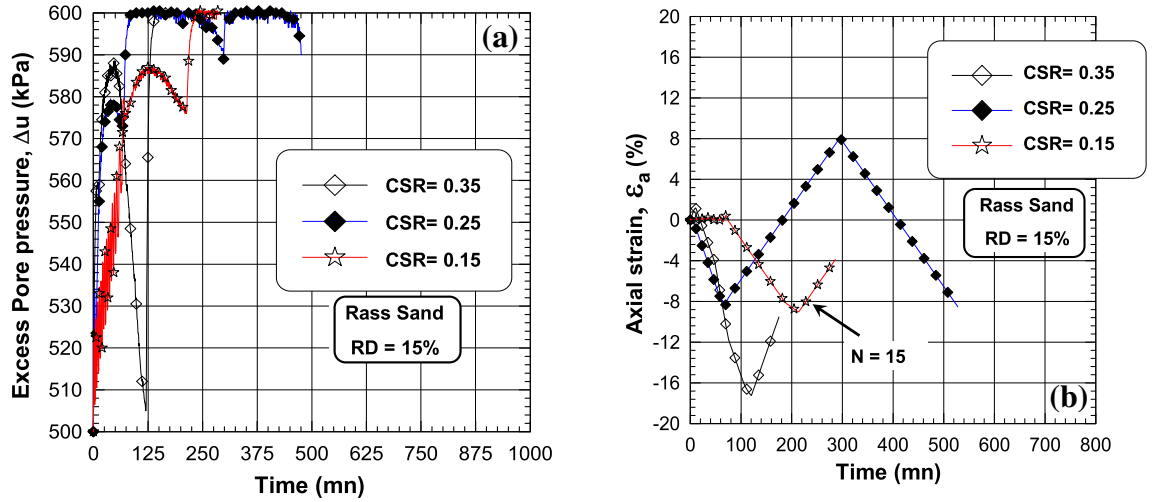

Fig. 7 Undrained cyclic tests on Rass sand (RD = 15 %, $p'_c = 100$ kPa). **a** Excess pore pressure (Δu) versus time, **b** axial strain (ε_a) versus time

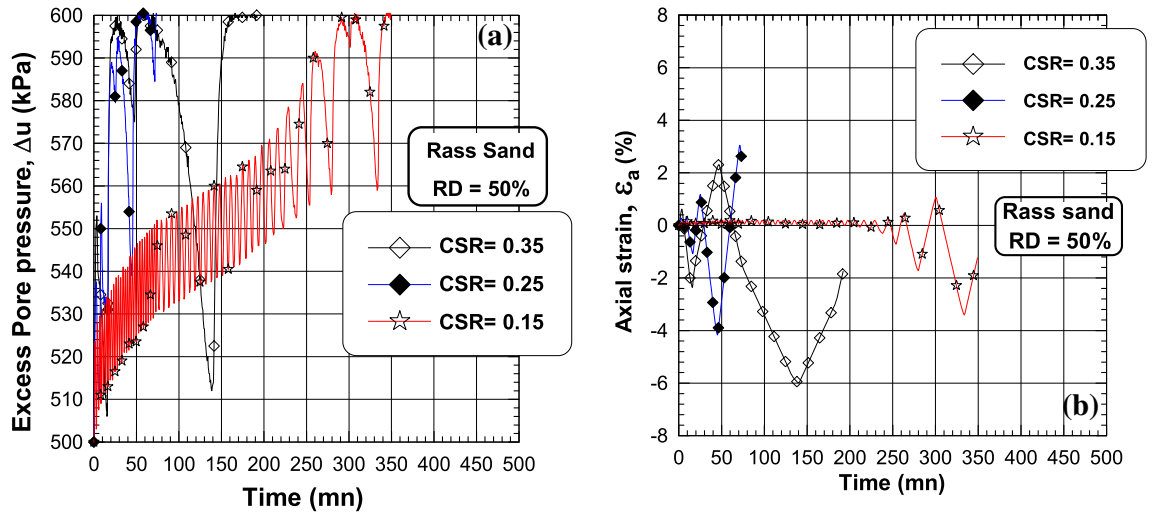

Fig. 8 Undrained cyclic tests on Rass sand (RD = 50 %, $p'_c = 100$ kPa). **a** Excess pore pressure (Δu) versus time, **b** axial strain (ε_a) versus time

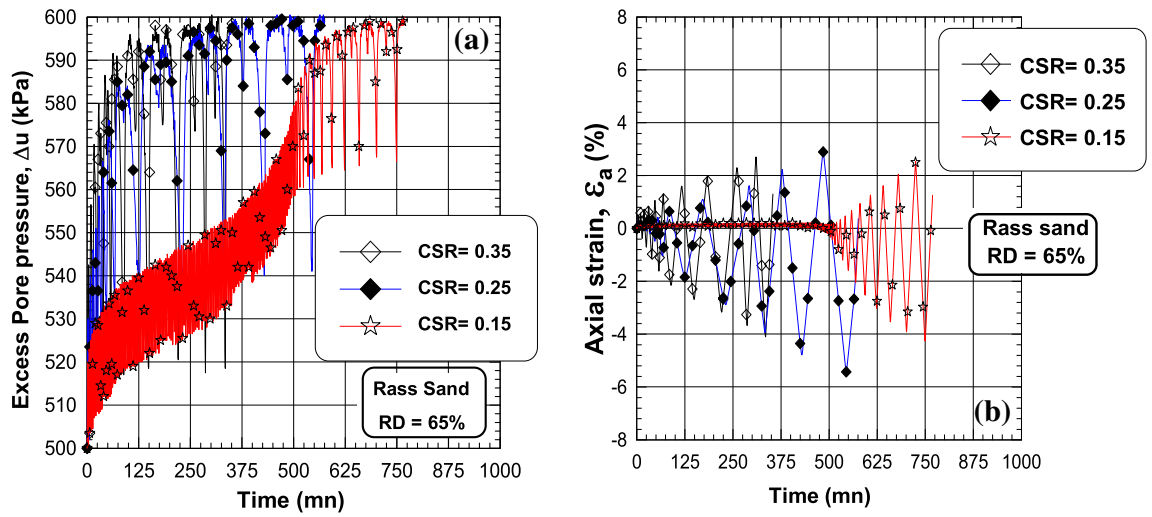

Fig. 9 Undrained cyclic tests on Rass sand (RD = 65 %, $p'_c = 100$ kPa). **a** Excess pore pressure (Δu) versus time, **b** axial strain (ε_a) versus time

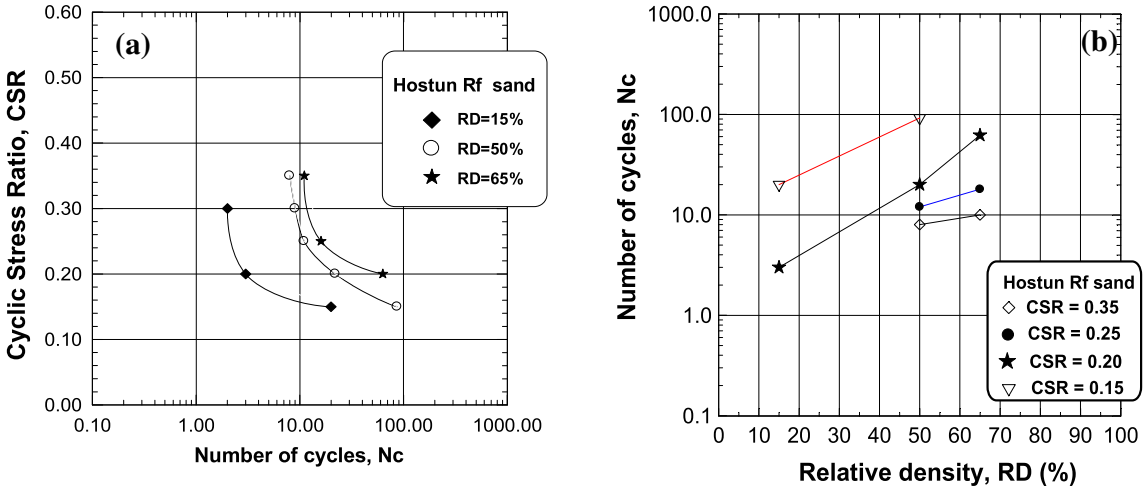

Fig. 10 Influence of relative density on the liquefaction potential of Hostun Rf sand. **a** Cyclic stress ratio (CSR) versus number of cycles (N_c), **b** number of cycles (N_c) versus relative density (RD)

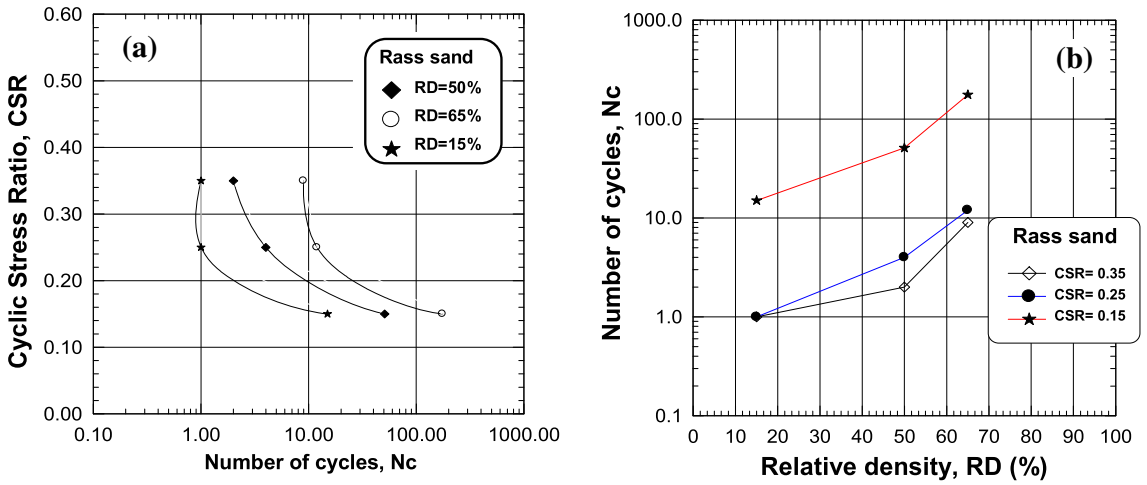

Fig. 11 Influence of relative density on the liquefaction potential of Rass sand. **a** Cyclic stress ratio (CSR) versus number of cycles (N_c), **b** number of cycles (N_c) versus relative density (RD)

after 12 cycles (Fig. 9a). Simultaneously, for RD = 15 %, the axial strain reached was 8 % in compression and 8.2 % in extension, inducing zero effective stress, and consequently leading to the condition of initial liquefaction (Fig. 7b) and 2.8 % in compression and 4 % in extension for RD = 50 % (Fig. 8b) and 3 % in compression and 5.6 % in extension for RD = 65 % (Fig. 9b).

The test with CSR = 0.15, took relatively long time to generate the excess pore pressure reaching a value of 530 kPa for RD = 15 %. Also, liquefaction was reached after fifteen cycles (Fig. 7a). However, for RD = 50 %, the test took a longer time to generate the excess pore pressure. As a consequence, liquefaction was reached after 51 cycles (Fig. 8a). For RD = 65 %, the test took a longer time to generate the excess pore pressure. As a consequence, liquefaction was reached after one hundred and 76 cycles (Fig. 9a). The axial strain reached was 0.4 % in compression and 9 % in extension (RD = 15 %) (Fig. 7b) and 0.8 % in compression and 3.5 % in extension for RD = 50 % (Fig. 8b) and 2.5 % in compression and 4.2 % in extension for RD = 65 % (Fig. 9b).

Figures 10, 11, and 12 summarize the all test results of the three tested sands (Hostun Rf, Rass, and Chlef sand). Figures 10a, 11a and 12a illustrate the influence of the relative density on the liquefaction potential of these sands. These test results show very clearly that the increase in relative density leads to an increases in the liquefaction resistance of these sands. We can note also that when the cyclic stress ratio (CSR) decreases consequently the number of cycle's increases. Figures 10b, 11b, and 12b show that the liquefaction resistance increases with the increase in the relative density and the decrease in the loading amplitude. The increase in relative density leads to an increase in the cycle's number required to liquefaction. Also, we note that the difference between the resistance of the Rass sand at a relative density

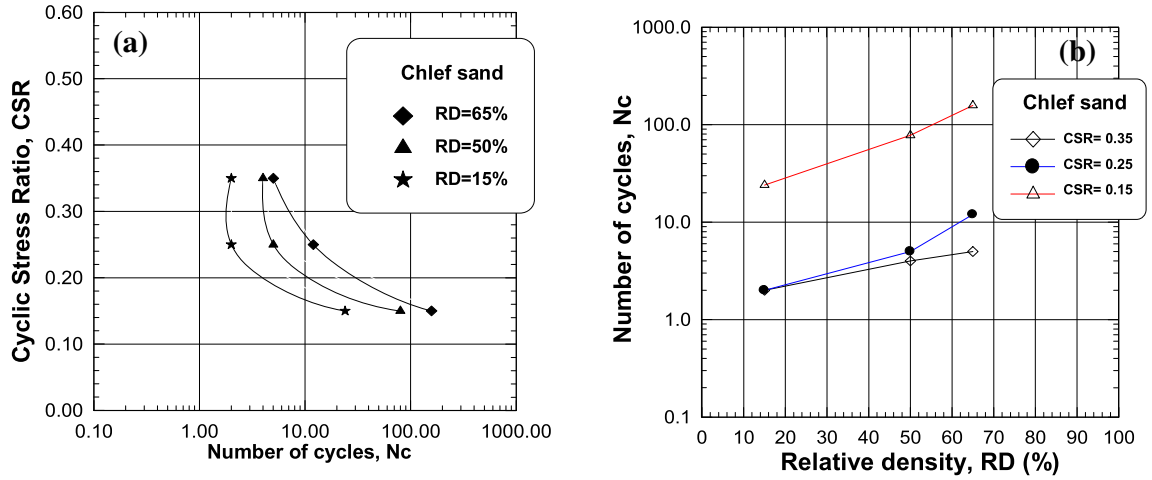

Fig. 12 Effect of relative density on the liquefaction potential of Chlef sand. **a** Cyclic stress ratio (CSR) versus number of cycles (N_c), **b** number of cycles (N_c) versus relative density (RD)

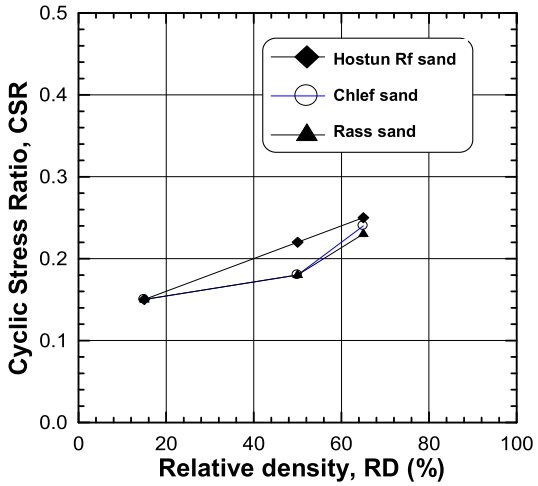

Fig. 13 Influence of relative density (RD) on the cyclic resistance (CSR) of the three tested sands (Chlef, Rass, and Hostun Rf)

of: RD = 50 % and RD = 65 % (Fig. 11b) is relatively higher in comparison with observed for Hostun Rf sand which the liquefaction resistance increases linearly with the increase in the relative density (Fig. 10b). Additionally, we note also that the difference between the resistance of the Chlef sand at a relative density of RD = 50 % and RD = 65 % (Fig. 12b) is very significant.

Figure 13 shows the influence of the relative density on liquefaction resistance defined by the loading amplitude that induces liquefaction after fifteen cycles for the three tested sands. This figure shows that the liquefaction resistance increases with the increase of relative density. We note also that cyclic liquefaction resistance was practically identical for the Rass sand and Chlef sand for the three selected relative densities. Additionally, we note also that the Hostun Rf sand posses a higher resistance than that of Rass and Chlef sands, when their relative density increases from 50 to 65 %. The reason for this increase in liquefaction resistance of the Hostun Rf sand is that the Hostun RF sand does not contain fines. However, Chlef sand and Rass sand, that were considered in this research study, contain low percentage of low plastic fines. Also, this is due to the angular shape of the sand particles of Hostun Rf sand which has a higher resistance than the rounded shape of Rass and Chlef sands' particles.

4 Conclusions

A series of undrained cyclic triaxial tests were carried out on three sands namely: Hostun Rf, Rass and Chlef sand. Undrained cyclic tests performed at initial relative densities of 15, 50 and 65 %, at a confining pressure of 100 kPa. The present laboratory study focuses on the effect of the initial density and the loading amplitude on the liquefaction potential of those sands. From the observed results, the following conclusions can be drawn:

Undrained cyclic tests show that the number of cycles to liquify tested samples increases with the decrease in the loading amplitude. It is also noted that the increase in the loading amplitude induces an important increase in the excess pore pressure; consequently, it accelerates liquefaction.

Increasing number of cycles, in tested sands, induced liquefaction. At a high relative density, the number of cycles necessary for the liquefaction becomes very important; specimens have exhibited a greater resistance to liquefaction and the increase of the relative density improves resistance to liquefaction of the three tested sands. Also, samples with medium and loose density are more vulnerable to liquefaction under high loading amplitude.

Increasing the initial relative density affects significantly the liquefaction potential of sand. It improves the resistance to liquefaction, and its effect becomes significant when the initial density increases from 50 to 65 %.

The cyclic liquefaction resistance was practically identical for the Rass and Chlef sands for the three selected relative densities. Additionally, the Hostun Rf sand has exhibited a higher resistance than that of Rass and Chlef sands, when their relative density increased from 50 to 65 %.

It was found that particles' shape have a significant effect on the cyclic liquefaction resistance. In essence, the angular shape of sand particles (Hostun Rf sand) exhibits a higher resistance than the rounded shape (Chlef and Rass sands).

The major outcome of this experimental study is that relative density has a significant effect on improving liquefaction resistance. For this purpose, it is highly recommended, for the sites presented in this study, to densify the soil in place before embarking on any construction-related activity, in order to increase liquefaction resistance of said sites.

Our results are in good agreement with those found in the literature on the influence of the relative density on the liquefaction potential of sands. Also from this experimental study, it was found that the angular shape of sand particles exhibits a higher resistance than the rounded shape one. For this purpose, it is also recommended to the practicing engineers designing and constructing on these specific sites to use the angular sand and to compact the soil in place to avoid the risk of liquefaction. It is recommended also to reinforce the sites presenting a risk of liquefaction for example by dynamic compaction reinforcement; also it is recommended to mapping the extents of liquefaction prone zone, and also it should be to mark in depth the levels of liquefy layers and in the lateral directions with different levels of liquefaction probability, and also it is recommended to mark all the sites subject to liquefaction phenomenon.

References

1. Mohamad, R.; Dobry, R.: Undrained monotonic and cyclic strength of sands. J. Geotech. Eng. **112**(10), 941–958 (1986)
2. Konrad, J.M.: Undrained response of loosely compacted sands during monotonic and cyclic compression tests. Géotechnique **43**(1), 69–89 (1993)
3. Hyodo, M.; Tanimizu, H.; Yasufuku, N.; Murata, H.: Undrained cyclic and monotonic triaxial behaviour of saturated loose sand. Soils Found. **34**(1), 19–32 (1994)
4. Tatsuoka, F.; Miura, S.; Yoshimi, Y.; Yasuda, S.; Makihara, Y.: Cyclic undrained triaxial strength of sand by a cooperative test program. Soils Found. **26**, 117–128 (1986b)
5. Finn, W.D.L.; Emery, J.J.; Gupta, Y.P.: A shaking table study of the liquefaction of saturated sands during earthquake. In: Proceedings 3rd European Symposium on Earthquake Engineering, pp. 253–262 (1970)
6. Belkhatir, M.; Arab, A.; Della, N.; Hanifi, M.; Schanz, T.: Influence of inter-granular void ratio on monotonic and cyclic undrained shear response of sandy soils. J. CRME (CRAS) **338**, 290–303 (2010)
7. Belkhatir, M.; Arab, A.; Della, N.: Liquefaction resistance of Chlef river silty sand: effect of low plastic fines and other parameters. Acta Polytech. Hung. **7**(2), 119–137 (2010)
8. Polito, C.P.; Martin, J.R.: Effects of non-plastic fines on the liquefaction resistance of sands. J. Geotech. Geoenviron. Eng. **127**(5), 408–415 (2001)
9. Della, N.; Arab, A.; Belkhatir, M.: Static liquefaction of sandy soil: An experimental investigation into the effects of saturation and initial state. Acta Mech. **218**(1-2), 175–186 (2010)
10. Belkhatir, M.; Schanz, T.; Arab, A.; Della, N.; Kadri, A.: Insight into the effects of gradation on the pore pressure generation of sand–silt mixtures. Geotechn. Test. J. **37**(5), 922–931 (2014)
11. Arab, A.: Comportement des Sols sous Chargement Monotone et Cyclique. Ph.D. dissertation, University of Sciences and Technology of Oran, Algeria (2008)
12. Krim, A.; Zitouni, Z.; Arab, A.; Belkhatir, M.: Identification of the behavior of sandy soil to static liquefaction and microtomography. Arabian J. Geosci. **6**(7), 2211–2224 (2013)
13. Benahmed, N.; Canou, J.; Dupla, J.C.: Structure initiale et propriétés de liquefaction statique d'un sable. J. CRME (CRAS) **332**, 887–894 (2004)
14. Colliat, J.L.: Comportement des matériaux granulaires sous forte contraintes, influence de la nature minéralogique du matériau étudié. Ph.D. dissertation, Institute of Mechanic of Grenoble, Grenoble, France (1986)
15. Fargeix, D.: Conception et réalisation d'une presse triaxiale dynamique-application à la mesure des propriétés des sols sous sollicitations sismiques. Ph.D. dissertation, Institute of Mechanic of Grenoble, Grenoble, France (1986)
16. Flavigny, E.; Desrues, J.; Palayer, B.: Le sable d'Hostun Rf. Rev. Fr. Géotech. **53**, 67–70 (1990)
17. Biarez, J.; Ziani, F.: Introduction aux lois de comportement des sables très peu denses. Rev. Fr. Géotech. **54**, 65–73 (1991)
18. Lancelot, L.; Shahrour, I.; Al Mahmoud, M.: Comportement du sable d'Hostun sous faibles contraintes. Rev. Fr. Géotech. **74**, 63–74 (1996)
19. Doanh, T.; Ibraim, E.; Matiotti, R.: Undrained instability of very loose Hostun sand in triaxial compression and extension. Part 1: experimental observations. Mech. Cohesive Frict. Mater. **2**, 47–70 (1997)
20. Al Mahmoud, M.: Etude en laboratoire du comportement des sables sous faibles contraintes. Ph.D. dissertation, University of Sciences and Technology of Lille, Lille, France (1997)
21. Hoque, E.; Tatsuoka, F.: Anisotropy in the elastic deformation of granular materials. Soils Found. **38**(1), 163–179 (1998)
22. Bishop, A.W.; Wesley, L.D.: A hydraulic triaxial apparatus for controlled stress path testing. Geotechnique **4**, 657–670 (1975)
23. Ladd, R.S.: Preparing test specimen using under compaction. Geotech. Test. J. GTJODJ **1**, 16–23 (1978)
24. Chan, C.K.: Instruction Manual, CKC E/P Cyclic Loading Triaxial System User's Manual. Soil Engineering Equipment Company, San Francisco (1985)
25. Lade, P.V.; Duncan, J.M.: Cubical triaxial tests on cohesionless soil. J. Soil Mech. Found. Div. ASCE **99**(SM10), 793–812 (1973)
26. Arab, A.; Shahrour, I.; Lancelot, L.: A laboratory study of liquefaction of partially saturated sand. J. Iber. Geol. **37**(1), 29–36 (2011)